Research Square

Preprints are preliminary reports that have not undergone peer review.
They should not be considered conclusive, used to inform clinical practice,
or referenced by the media as validated information.

Matric-potential-dependent capillary loading on a cell-sized particle: implications for Bacillus subtilis swarming

Irakli Gudavadze

irakli.gudavadze@utexas.edu

The University of Texas at Austin

Research Article

Keywords: Bacillus subtilis, bacterial swarming, agar matric potential, capillary force, Young–Laplace equation, surfactin

Posted Date: November 23rd, 2026

DOI: https://doi.org/10.21203/rs.3.rs-11721325/v1

License: This work is licensed under a Creative Commons Attribution 4.0 International License.
Read Full License

Additional Declarations: No competing interests reported.

Matric-potential-dependent capillary loading on a cell-sized particle: implications for Bacillus subtilis swarming

Article type: Original Research (theoretical/computational study)

Author: Irakli Gudavadze

Affiliation: The University of Texas at Austin

Corresponding author: Irakli Gudavadze; irakli.gudavadze@utexas.edu

ORCID: 0000-0002-6624-0918

Acknowledgements: None

Abstract

Swarming of Bacillus subtilis depends on the hydration state of the supporting agar, but the consequences of agar matric potential for cell-scale capillary loading are poorly quantified. We solve the full nonlinear, axisymmetric Young–Laplace equation for a 1-µm-diameter, perfectly wetting sphere touching a rigid agar surface, prescribing pressure from a published agar concentration–matric-potential relation. In the idealized finite-bridge geometry with zero exterior film thickness and zero contact angles on both sphere and substrate, increasing agar concentration from 0.5% to 1.0% raises the predicted downward normal force from 97.64 to 112.76 nN (15.48%) at 72 mN/m. At 27 mN/m, a surface tension achieved by purified surfactin, forces are 40.67 and 47.62 nN (17.09%). The force difference is primarily due to shifts in contact-line geometry, not the direct pressure contribution. A sensitivity analysis shows that a 5° substrate contact angle reduces the relative increase to 1.16% at 72 mN/m, highlighting dependence on ideal wetting. These stationary calculations propose a testable mechanism for enhanced mechanical confinement on concentrated agar but do not demonstrate equilibrium stability or a critical threshold for swarming arrest.

Keywords: Bacillus subtilis; bacterial swarming; agar matric potential; capillary force; Young–Laplace equation; surfactin

Introduction

Collective surface migration of *Bacillus subtilis* couples flagellar propulsion, dense cell organization, interfacial hydration, and surface-active chemistry. In a classic characterization of undomesticated strain 3610, Kearns and Losick (Kearns and Losick 2003) observed surface

spreading on 0.5% and 0.7% agar, whereas spreading at 1.0% was restricted under the tested medium and incubation conditions. Agar concentration is therefore a convenient experimental control, but it is not itself a molecular explanation: it simultaneously changes water potential, hydraulic permeability, gel mechanics, and possibly microscopic wetting. The concentration threshold is also strain- and protocol-dependent and should not be regarded as a universal 0.8% transition (Kearns and Losick 2003; Yang et al. 2017).

Water availability and interfacial forces are established ingredients in swarming. In *Pseudomonas aeruginosa*, increasing agar concentration or adding osmolytes suppressed colony expansion while additional surfactant facilitated it (Yang et al. 2017). In *B. subtilis*, surfactin can lower local surface tension and trigger the spreading of a liquid layer over which motile cells migrate (Ke et al. 2015). Swarming of several pseudomonads is sensitive to changes in substrate matric water potential smaller than 1 kPa (Dechesne and Smets 2012). Yet these biological observations do not uniquely specify the capillary forces experienced by an individual surface-associated cell, nor do they distinguish equilibrium mechanical confinement from the kinetics of water replenishment.

Anno, Ishida, and Nagano (Anno et al. 1999) measured a concentration-dependent matric potential for agar gels. Independently, Gudavadze and Florin (Gudavadze and Florin 2022) computed normal forces on spherical particles protruding from thin liquid films with nonlinear Young–Laplace theory. Recent experiments also establish that bacterial menisci can mediate intercellular organization in partially hydrated colonies (Black et al. 2025). Here, we combine the *measured substrate state variable* in (Anno et al. 1999) with an idealized capillary-force calculation to ask a specific question: how much could the matric-potential difference between 0.5% and 1.0% agar change the normal load on an isolated, wetting, cell-sized object?

We deliberately isolate this proposed equilibrium mechanism; its pressure boundary condition and finite wetted domain require experimental validation. The agar is treated as rigid, the particle is spherical and fixed in place, both contact angles are set to zero, the exterior liquid film is dry at finite radial distance, and gravity is neglected. We calculate both the 72 mN/m water reference and a 27 mN/m surfactin scenario; the latter value has been reported for purified surfactin (Yeh et al. 2005) but must not be interpreted as the measured surface tension of an actual swarm. Because the normal-load-to-motility relationship is presently unmeasured, we present swarming arrest as a *testable interpretation* rather than a numerical prediction of a critical agar concentration.

Materials and methods

Physical geometry and thermodynamic input

A rigid sphere with radius $R = 0.5\,\mu$m makes point contact with a perfectly planar, infinitely stiff gel at $z = 0$; its center lies at $z = R$. A liquid bridge connects a contact line on the sphere to a circular contact line of radius b on the gel. The undisturbed film thickness *outside the finite bridge* is zero. Both particle–water and gel–water Young contact angles are fixed at $0°$ for the principal calculation; an additional contact-angle sensitivity analysis varies the gel angle from $0°$ to $30°$. No external force is applied to select the meniscus; its stationary geometry is selected mathematically by the prescribed pressure and wetting boundary conditions. The sphere is held at its specified height, and we report the capillary force needed to hold it there.

We use the measured agar fit from Anno et al. (Anno et al. 1999),

$$\Psi_m(C) = -0.153\,C^{1.91}\ \text{kPa},$$

where C is the **numerical mass percentage** (e.g., $C = 0.5$ for 0.5 wt% agar). Importantly, Anno et al. obtained this relation using the **gel concentration after equilibration and drainage** in their water-potential experiments, not necessarily the nominal agar percentage used to prepare an inoculated swarming plate. Equating these concentration labels is an additional modeling assumption and should be tested experimentally. In the idealized model, the liquid-minus-air pressure difference is assumed to equal the gel matric potential, $\Delta p = p_L - p_A = \Psi_m(C) < 0$. This equality assumes chemical equilibrium, a pore-water pressure whose matric contribution can be represented by $p_L - p_A$, matched freely dissolved solute contributions between gel pore water and meniscus, and an environment compatible with the imposed liquid chemical potential. It is a constitutive hypothesis, **not a direct experimental measurement of pressure in a swarming colony**. The water-availability correlation was obtained with a particular gel preparation; its extrapolation to nutrient-rich swarming plates is an important source of uncertainty. No gel-concentration-dependent change in particle contact angle, agar contact angle, or surface tension is assumed except in the separate surfactin sensitivity calculation.

The initial surface tension is $\gamma = 72\ \mathrm{mN\,m^{-1}}$. To represent biosurfactant action, we repeat the calculation at $\gamma = 40, 30, 28,$ and $27\ \mathrm{mN\,m^{-1}}$. Yeh, Wei, and Chang (Yeh et al. 2005) measured a reduction from approximately 72 to 27 mN/m for purified surfactin; the present 27 mN/m simulation is an endpoint sensitivity calculation, with contact angles held fixed even though real surfactin can also change wetting chemistry.

Full nonlinear Young–Laplace model

We parameterize the axisymmetric liquid–air meridian by arc length s, radial position $r(s)$, height $z(s)$, and tangent inclination $\psi(s)$ with respect to the positive radial axis. With the sign

convention $\Delta p = p_L - p_A$ and the interface orientation defined in Fig. 1, the complete, **nonlinear** equations are

$$\frac{dr}{ds} = \cos\psi, \qquad \frac{dz}{ds} = \sin\psi, \qquad \frac{d\psi}{ds} = \frac{\Delta p}{\gamma} - \frac{\sin\psi}{r}.$$

No linearization of curvature or small-slope approximation is used. The spherical contact line is parameterized by its filling angle α measured upward from the sphere's lowest point. For a zero particle contact angle,

$$r_p = R\sin\alpha, \qquad z_p = R(1 - \cos\alpha), \qquad \psi_p = \alpha.$$

At the gel-side contact line, perfect wetting and the zero-height plane give

$$r = b, \qquad z = 0, \qquad \psi = \pi.$$

The unknown α and b are determined by satisfying Eqs. 2–4, with the sphere remaining tangent to the dry plane at $r = 0$. To avoid numerical stiffness in the long, shallow bridge, we integrate in ψ, using $d(r, z)/d\psi = (\cos\psi, \sin\psi)/(\Delta p/\gamma - \sin\psi/r)$, and solve the scalar condition $z(\pi) = 0$ for α. All dimensional quantities are restored with R.

Equation 2 has the exact first integral

$$r\sin\psi - \frac{\Delta p}{2\gamma} r^2 = A.$$

The constant A is determined independently at each boundary, providing a stringent numerical check. In this finite-bridge model the pressure does not vary with z, because gravity is neglected. The associated Bond number $\rho g R^2/\gamma$ is 3.4×10^{-8} at 72 mN/m and approximately 9.1×10^{-8} at 27 mN/m; hence gravitational pressure variation across the **micrometer-scale height** is negligible compared with the tens-to-hundreds of pascals used here. This model is distinct from a sphere on a

liquid half-space, for which gravity can set the far-field meniscus even when the local Bond number is small (Gudavadze and Florin 2022).

Axial capillary-force calculation and validation

We define positive $F_{\downarrow}$ as the downward force exerted on the sphere by the liquid. The contact-line surface tension and pressure contributions are

$$F_\gamma = 2\pi R\gamma \sin^2\alpha, \qquad F_p = -\Delta p\, \pi R^2 \sin^2\alpha.$$

The total normal load is therefore

$$F_{\downarrow} = F_\gamma + F_p.$$

For the zero-angle gel boundary, Eq. 5 also gives the independent identity

$$F_{\downarrow} = \pi b^2 |\Delta p|.$$

We require agreement of Eqs. 7 and 8 to relative accuracy better than 10^{-8}, as well as constancy of the first integral along each numerical profile. The code uses SciPy's high-order ODE integrator and Brent root finding with stringent numerical tolerances. Neither agar concentration nor surface tension is fitted to observed swarming velocities.

Role of computational assistance and verification

OpenAI ChatGPT was used in the preparation of manuscript prose and in development of Python scripts used for the nonlinear meniscus calculations. The numerical results were checked against a separately implemented radial-quadrature solution and the exact first integral. The corresponding author must review the scripts, scientific interpretations, and all statements before submission and assumes responsibility for the submitted work.

Results

Concentration-dependent changes in an idealized capillary bridge

Equation 1 gives $\Psi_m(0.5) = -40.712$ Pa and $\Psi_m(1.0) = -153.000$ Pa. The concentration shift is therefore 112.288 Pa. At $\gamma = 72$ mN/m, the nonlinear solutions predict a wetting radius b of 27.63 µm for 0.5% agar and 15.32 µm for 1.0% agar (Fig. 1). The more negative matric potential is associated with a **smaller wetted area on the gel** but a change in the sphere filling angle from 138.93° to 135.10°, increasing the vertical contact-line force (Table 1).

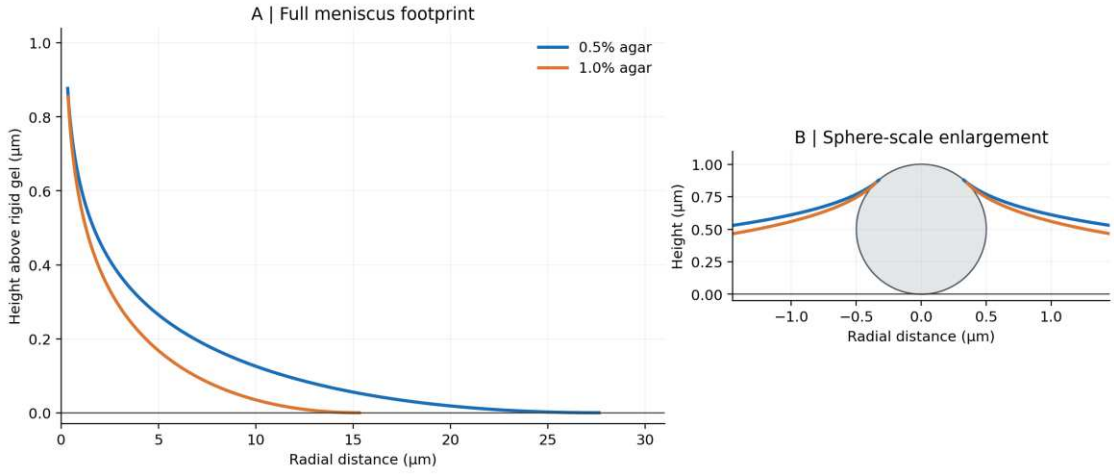

Fig. 1. Nonlinear equilibrium meniscus for a 1-µm spherical particle on 0.5% and 1.0% idealized agar at a fixed surface tension of 72 mN/m. The left panel shows the complete wetting footprint, and the right panel displays the circular particle cross-section at equal spatial scales. Both curves meet the spherical particle tangentially. The black baseline represents an infinitely stiff agar surface. These are calculated stationary profiles, not measured wetting patterns.

Table 1. Nonlinear meniscus geometry and axial capillary loading at 72 mN/m. Matric potentials are obtained from Eq. 1; all other quantities are numerical model predictions.

Quantity	0.5% agar	0.7% agar	0.8% agar	1.0% agar

Quantity	0.5% agar	0.7% agar	0.8% agar	1.0% agar
Matric potential (Pa)	−40.712	−77.416	−99.906	−153.000
Sphere filling angle (deg)	138.931	137.192	136.442	135.101
Gel wetting radius (μm)	27.630	20.727	18.502	15.316
Surface-tension force (nN)	97.626	104.452	107.408	112.700
Direct pressure force (nN)	0.0138	0.0281	0.0373	0.0599
Total downward force (nN)	**97.640**	**104.480**	**107.445**	**112.760**

The force rises from 97.640 nN at 0.5% to 112.760 nN at 1.0%, corresponding to

$$\frac{F_{\downarrow}(1.0) - F_{\downarrow}(0.5)}{F_{\downarrow}(0.5)} \times 100\% = 15.4849\%.$$

The surface-tension term accounts for virtually all of the absolute force, while the direct pressure force contributes only 0.014–0.060 nN across the endpoints. Thus, the literature-derived pressure input changes the force **mostly by moving the equilibrium contact line**, not by its direct action over the small projected area of the sphere. Equations 7 and 8 agree to at least eight significant figures for all reported parameter combinations.

Surfactin-associated reduction in surface tension to 27 mN/m

Lowering surface tension decreases the computed normal capillary force (Fig. 2). With the experimentally attainable purified-surfactin endpoint of $\gamma = 27$ mN/m (Yeh et al. 2005), the force becomes 40.667 nN at 0.5% agar and 47.617 nN at 1.0% agar. Thus,

$$\Delta F_{27} = 6.950\ \text{nN}, \qquad \frac{\Delta F_{27}}{F_{27}(0.5)} \times 100\% = 17.0909\%.$$

For a fixed agar concentration, these forces are approximately 58% lower than the corresponding 72 mN/m forces, even though the *relative* increase with gel concentration remains close to 15–

17%. The relative difference is not exactly independent of γ: changing surface tension alters the dimensionless pressure $\Delta pR/\gamma$, thereby shifting the meniscus contact positions.

Table 2. Endpoint force comparison under surface-tension sensitivity. Each row separately solves the full nonlinear boundary-value problem with both contact angles fixed at zero.

Surface tension (mN/m)	$F(0.5\%)$ (nN)	$F(1.0\%)$ (nN)	Increase (nN)	Increase (%)
72	97.640	112.760	15.119	15.485
40	57.701	67.176	9.475	16.421
30	44.659	52.209	7.551	16.908
28	42.002	49.154	7.152	17.027
27	**40.667**	**47.617**	**6.950**	**17.091**

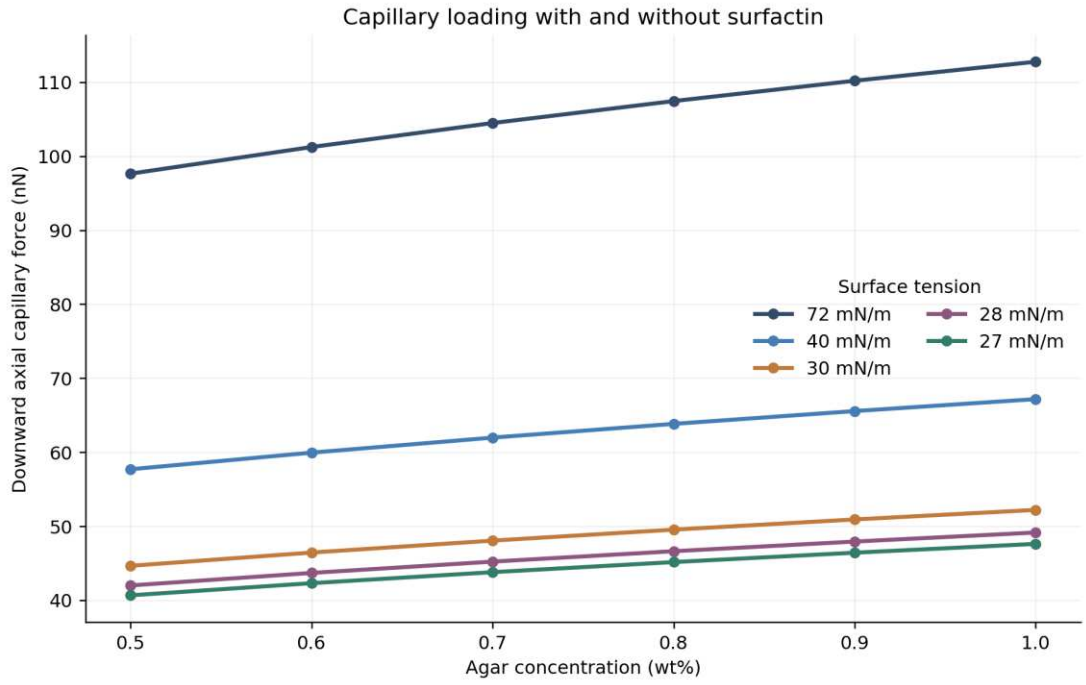

Fig. 2. Calculated normal capillary force against agar concentration for five prescribed liquid–air surface tensions. The 27 mN/m endpoint represents a purified-surfactin scenario; surface tension in an actual swarm was not measured.

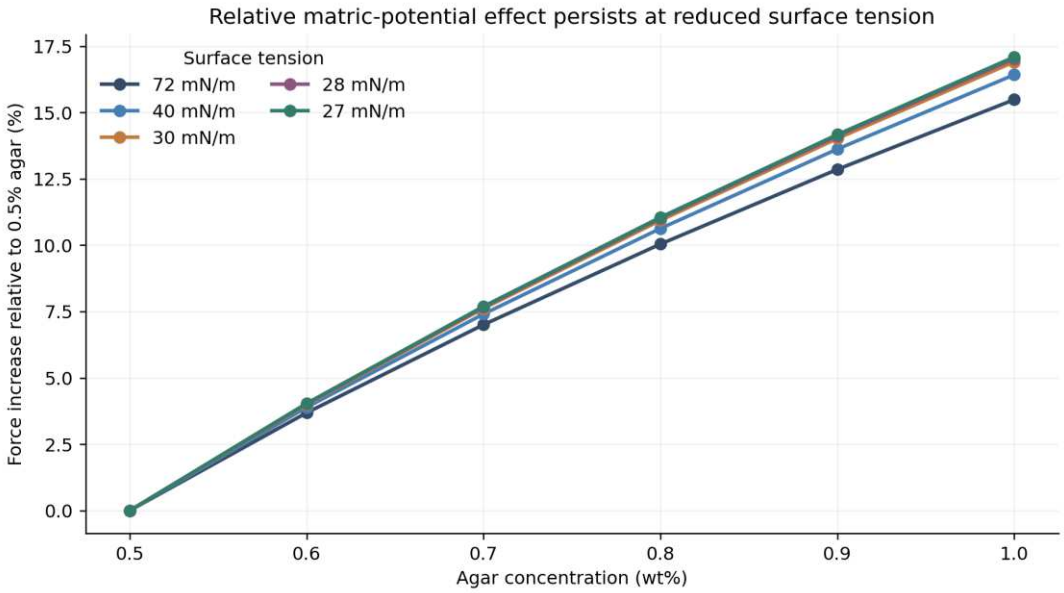

Fig. 3. Percentage increase in capillary load relative to the force at 0.5% agar for each fixed surface tension. The dependence is continuous; the model has no intrinsic discontinuity near 0.7–0.8% agar.

Contact-angle sensitivity and robustness of the central comparison

Because the zero contact angle on agar is an idealization rather than a measured property of the swarming plates, we repeated the stationary nonlinear calculation with a fixed but nonzero gel–water Young angle θ_g while maintaining $\theta_p = 0°$. The gel boundary condition becomes $\psi_g = \pi - \theta_g$. At that boundary, Eq. 5 implies the generalized force identity

$$F_{\downarrow} = 2\pi\gamma b \sin\theta_g + \pi b^2 |\Delta p|.$$

The zero-angle formula in Eq. 8 is recovered when $\theta_g = 0$. The continuation is computed with independent radial quadrature using the exact first integral, rather than relying on the original tangent-angle integrator. This extension is deliberately a **boundary-condition sensitivity test**, not an empirical claim that agar gels have a particular contact angle.

Table 3. Sensitivity of the relative force increase from 0.5% to 1.0% agar to the gel–water contact angle. The sphere contact angle remains zero. The complete sweep from 0° to 30° is provided as supplementary data.

Agar contact angle	Force at 0.5%, 72 mN/m (nN)	Force at 1.0%, 72 mN/m (nN)	Increase at 72 mN/m	Increase at 27 mN/m
0°	97.640	112.760	15.49%	17.09%
1°	108.699	117.786	8.36%	12.79%
2°	121.372	126.415	4.15%	8.14%
5°	147.586	149.301	1.16%	2.83%

At 72 mN/m, changing only θ_g from 0° to 5° reduces the concentration-dependent force enhancement by more than an order of magnitude, even though the absolute force at each concentration increases. The main 15.48% figure is therefore a **conditional perfect-wetting result**, not a contact-angle-independent prediction for *B. subtilis* cultures. In particular, the experiment must determine whether the agar contact line is nearly perfectly wetted, and whether surfactin changes its angle, before this mechanism can be assigned a quantitative contribution to swarming arrest.

The model does not automatically generate a motility threshold

The force–concentration curves are smooth (Figs. 2 and 3) within the fixed-zero-angle model. The contact-angle sensitivity in Table 3 additionally shows that the size of the predicted concentration effect is strongly dependent on the wetting boundary condition. For example, at 72 mN/m, the force increases from 104.48 nN at 0.7% agar to 107.45 nN at 0.8%, a 2.84% change. At 27 mN/m, the same step changes the force from 43.80 nN to 45.16 nN, or 3.12%. No abrupt change in the static solution occurs at these concentrations. Therefore, experimental cessation of swarming within such an interval requires an additional biological or physical *threshold* (for example,

insufficient propulsive force relative to an effective resisting load) rather than a singularity in the capillary solution.

Discussion

Mechanistic interpretation: a proposed resistance to motion

Under the idealized conditions, concentrated agar has a more negative matric potential, a smaller stationary gel-side wetting radius, and a stronger capillary attraction pulling a sphere toward the substrate. If normal loading increases cell–substrate resistance, this could make collective movement more difficult. One phenomenological expression for a putative threshold is

$$F_{\mathrm{drive}} \leq F_{\mathrm{other}} + \mu_{\mathrm{eff}} F_{\downarrow},$$

where F_{drive} is effective flagellar/collective driving, F_{other} includes resistance not proportional to the capillary normal force, and μ_{eff} is an **unknown** effective coupling coefficient. Equation 12 is a *proposed constitutive test*, not a measured law for bacteria on wet agar. For a freely lubricated cell that does not touch the substrate, simple dry-friction scaling may fail; hydrodynamic resistance, liquid-film thickness, and capillary pinning should instead be measured explicitly. We therefore refrain from assigning a critical agar percentage from the predicted normal force alone.

The surfactin calculation provides a second potentially falsifiable implication: sufficiently strong surface-tension reduction decreases absolute normal loading, even if the matric-potential dependence persists. This is mechanistically compatible with experimental evidence that surfactin changes liquid redistribution and swarming morphology (Ke et al. 2015), but surfactin also alters dynamic contact angles, Marangoni stresses, and secretion-dependent surface flow. Our calculations isolate only the γ dependence while retaining the same idealized contact angles and

pressure fit. A bacterial swarm need not operate at the purified-surfactin limit of 27 mN/m (Yeh et al. 2005).

Relevance to physical cell–substrate interactions

The present model addresses a surface-normal component of the mechanical environment of motile bacteria. It does not directly solve the equations of bacterial propulsion. The mechanistic hypothesis is that an increase in normal capillary load could decrease cell–substrate separation, strengthen contact-mediated resistance, or modify lubrication during flagellar motion. Each pathway entails additional physics and may be insignificant in a swarm whose cells remain separated from the substrate by a continuous film. Because the finite wetted footprint predicted here extends over many cell diameters, collective multi-particle geometry and the connectivity of the surface liquid are likely to be decisive.

Relation to prior physical studies

Prior studies established the importance of water films, surface-tension effects, and substrate hydration in microbial movement (Yang et al. 2017; Ke et al. 2015; Dechesne and Smets 2012; Araujo et al. 2019). Gudavadze and Florin (Gudavadze and Florin 2022) solved related capillary-force problems for particles in thin films. Black and colleagues (Black et al. 2025) demonstrated capillary-mediated organization of rod-shaped bacteria in confined water layers. Our narrower contribution is a **quantitative map from a published agar matric-potential curve to a stationary normal-load prediction**, including surfactin sensitivity. This is not presented as a new numerical Young–Laplace method, an experimentally validated universal mechanism, or an explanation of collective rheology. The distinction from recent capillary-organization studies is its

explicit use of gel *concentration-dependent water potential* to predict a change in the *vertical* particle force.

Assumptions that limit inference from the calculated 15–17% increase

Strong contact-angle sensitivity. Table 3 shows that a modest departure from zero gel contact angle can nearly erase the predicted 15–17% concentration effect. The actual equilibrium or apparent contact angle of a hydrated, heterogeneous agar surface has not been measured here, and contact-line pinning can lead to apparent angles distinct from the ideal Young angle. This is a central uncertainty, not a minor perturbation.

Unknown stability of the finite bridge. The boundary conditions select a finite, stationary Young–Laplace meniscus with complete wetting on both solids and a dry exterior. Complete wetting can instead favor a precursor film and a non-sharp outer contact line, and a stationary capillary solution need not be the global minimum of an appropriate grand potential. In particular, the 15–28 µm wetting footprints vastly exceed the 0.5 µm particle radius. These results require an experimental or free-energy validation of the finite-bridge state before its force is treated as a directly observable equilibrium load.

Independent-particle approximation. Real *B. subtilis* is rod-shaped and often closely packed in dynamic rafts. Neighboring menisci overlap at separations much smaller than our calculated footprint radii; superposition of isolated-sphere forces would be invalid. Particle shape, cell–cell capillarity, and surface lubrication could change both sign and magnitude of effective movement resistance (Gudavadze and Florin 2022; Black et al. 2025).

Concentration calibration and potential uncertainty. The Anno et al. correlation uses an equilibrated agar concentration measured after drainage in a particular experimental system. It

cannot automatically be assigned to a nominal 0.5% or 1.0% nutrient agar plate, and the original measurements do not quantify the uncertainty in the present force prediction. The numerical precision of Tables 1–3 represents solver accuracy, not experimental confidence.

Matric versus osmotic contributions. Equation 1 describes one study of agar matric potential, not the total water potential of every nutrient medium. The assignment $\Delta p = \Psi_m(C)$ assumes matched pore-water/meniscus solute contributions and a compatible vapor environment. It must not be confused with an assumed bacterial osmotic pump or with hydraulic permeability. The latter determines supply kinetics and does not appear in the stationary equation. Changes in nutrient concentration or evaporation could dominate the actual water chemical potential in a colony.

Gravity and the far field. Gravity is negligible over the submicrometer meniscus height in the present finite-bridge model. The result does **not** describe a sphere contacting an infinite water half-space, in which gravity—even at small local Bond number—can control the distant interface (Gudavadze and Florin 2022). The outer boundary conditions must not be interchanged when comparing these geometries.

Biological causality. A normal capillary force has been computed for an immobilized sphere, not measured on moving bacterial cells. A 15.48% increase is not automatically sufficient to stop swarming, and there is no prediction of the biological response without independent force–velocity measurements. The experimentally observed agar threshold may reflect dynamic water replenishment, changed cell physiology, contact-line hysteresis, or several coupled mechanisms.

Experiments that can discriminate the hypothesis

The most direct test uses the same agar formulation across 0.5%, 0.7%, 0.8%, and 1.0% while controlling medium composition and humidity. First, independently measure the matric water potential or water activity, contact angles, and surface tension of the cell-free surface and of the colony liquid. Second, use monodisperse hydrophilic microspheres on the gels to measure the meniscus profile and its force, including whether the liquid forms a finite contact line or a precursor film. Third, image *B. subtilis* flagellar activity, cell–surface separation, migration speed, and film thickness while changing surfactin abundance at fixed gel concentration. A measurable monotone increase in normal load at fixed interfacial chemistry, together with an independently established loading–motility relationship, would support the proposed mechanism. A constant force, lack of an admissible finite meniscus, or lack of correlation between loading and motility would constrain or falsify the present equilibrium explanation.

Conclusion

Within the stationary finite-bridge model **with both contact angles fixed at zero**, the full nonlinear Young–Laplace calculation predicts that changing the agar matric potential from −40.712 Pa (0.5%) to −153.000 Pa (1.0%) increases the downward axial capillary force from 97.64 to 112.76 nN (**15.48%**) at 72 mN/m. Repeating the calculation at **27 mN/m**, a reported purified-surfactin endpoint, produces **40.67 and 47.62 nN**, respectively (**17.09%**). The central mathematical observation is a change in the *surface-tension force through altered wetting geometry*, not a large direct pressure load. Critically, the relative force enhancement falls to 1.16% at 72 mN/m and 2.83% at 27 mN/m if the gel angle is 5°, so the main result is quantitatively fragile to the assumed wetting condition. The model makes a quantitative and testable connection

between gel water potential and potential confinement of surface-associated bacteria; it does not yet establish that this mechanism causes swarming arrest. Validating the finite meniscus, linking load to motility, and accounting for collective wetting are necessary before making that causal claim.

Statements and declarations

Competing interests. The author declares no competing interests.

Funding. No external funding supported the work

Author contributions. Irakli Gudavadze: conceptualization, model formulation, formal analysis, software verification, interpretation, and manuscript preparation

Data availability. All results are generated by the accompanying Python scripts from the explicitly stated parameters and the published matric-potential relationship. CSV results, numerical profiles, plotting scripts, and independent cross-checks are supplied at https://doi.org/10.5281/zenodo.24024964

Ethics approval. Not applicable: this is a theoretical study without new human or animal data or experiments.

References

Anno T, Ishida T, Nagano T (1999) Matric potential and overburden potential in gels for plant tissue culture. Environment Control in Biology 37:129–135. https://doi.org/10.2525/ecb1963.37.129

328 Araujo G, Chen W, Mani S, Tang JX (2019) Orbiting of flagellated bacteria within a thin fluid
329 film around micrometer-sized particles. Biophysical Journal 117:346–354.
330 https://doi.org/10.1016/j.bpj.2019.06.005

331 Black ME, Fei C, Alert R, Wingreen NS, Shaevitz JW (2025) Capillary interactions drive the self-
332 organization of bacterial colonies. Nature Physics 21:1444–1450. https://doi.org/10.1038/s41567-
333 025-02965-y

334 Dechesne A, Smets BF (2012) Pseudomonad swarming motility is restricted to a narrow range of
335 high matric water potentials. Applied and Environmental Microbiology 78:2936–2940.
336 https://doi.org/10.1128/AEM.06833-11

337 Gudavadze I, Florin E-L (2022) Normal capillary forces on a spherical particle protruding from a
338 thin liquid film and its application to swarming bacteria. Colloids and Surfaces A:
339 Physicochemical and Engineering Aspects 636:128176.
340 https://doi.org/10.1016/j.colsurfa.2021.128176

341 Ke W-J, Hsueh Y-H, Cheng Y-C, Wu C-C, Liu S-T (2015) Water surface tension modulates the
342 swarming mechanics of Bacillus subtilis. Frontiers in Microbiology 6:1017.
343 https://doi.org/10.3389/fmicb.2015.01017

344 Kearns DB, Losick R (2003) Swarming motility in undomesticated Bacillus subtilis. Molecular
345 Microbiology 49:581–590. https://doi.org/10.1046/j.1365-2958.2003.03584.x

346 Yang A, Tang WS, Si T, Tang JX (2017) Influence of physical effects on the swarming motility of
347 Pseudomonas aeruginosa. Biophysical Journal 112:1462–1471.
348 https://doi.org/10.1016/j.bpj.2017.02.019

349 Yeh M-S, Wei Y-H, Chang J-S (2005) Enhanced production of surfactin from Bacillus subtilis by
350 addition of solid carriers. Biotechnology Progress 21:1329–1334.
351 https://doi.org/10.1021/bp050040c